A Network Flow Approach to Battery Electric Bus Scheduling

Justin Whitaker, Greg Droge, Matthew Hansen, Daniel Mortensen, Jacob Gunther

***Abstract*—A major challenge to adopting battery electric buses into bus fleets is the scheduling of the battery charging while considering route timing constraints and battery charge. This work develops a scheduling framework to balance the use of slow and fast chargers assuming the bus routes and charger locations are fixed. Slow chargers are utilized when possible to lower the cost of charging and fast chargers are used when needed to meet timing constraints and to ensure a sufficient charge for route execution. A directed, acyclic graph is used to model the available charge times for buses that periodically return to the station to pick up passengers and to recharge its battery. A constrained network flow Mixed-Integer Linear Program (MILP) problem is formulated to optimize the scheduling of chargers as well as to determine the number of chargers required to meet battery state of charge thresholds. Using a randomly generated route schedule for thirty buses, results are presented that demonstrate the ability of the proposed method to find optimal charging plans while considering peak time charging costs and allowing for fixed and variable numbers of chargers.**

I. Introduction

Battery electric buses (BEBs) are being adopted in various markets in an effort to reduce air pollution, decrease vehicle noise, and lower maintenance costs [1], [2], [3], [4]. However, from a "refueling" perspective, energy storage in batteries requires more time than for combustible-fuel energy storage systems. Instead of minutes to fully refill the combustible-fuel energy storage, it can take the better part of an hour for a fast battery charge and several hours for a slow battery charge [4]. Consideration of bus route schedules and limited numbers of chargers provides additional complexity for determining when and how much to charge each bus. Furthermore, battery health is a concern due to the expense of the battery [5] and is adversely affected by fast-charging [6]. This paper presents a scheduling framework for a BEB fleet that must share a number of slow and fast chargers. It provides the ability to consider first order charging dynamics and fixed bus schedules while ensuring required battery state-of-charge thresholds are met.

Recent research seeks to enable BEB fleet deployment by solving two problems: providing BEB scheduling (when to charge, at which charger) and determining BEB infrastructure (charger placement, route design). Much attention has been given to solving both problems simultaneously [7], [8], [9], [10]. Additional variations in addressing the infrastructure include determining which existing buses should be replaced by a BEB [11], assignments of buses to routes [12], and determining locations of fast wireless chargers along the routes [13], [14]. The added complexity of considering both the BEB charge scheduling and the infrastructure problems necessitates simplifications for sake of computation.

Two such simplifications are common. First, only fast chargers are utilized in planning [7], [8], [10], [11], [12], [13], [14], [15]. Second, singificant simplifications to the charging models are made. Some approaches assume full charge [7], [10], [11], [14]. Others have assumed that the charge received is proportional to the time spent on the charger [12], [13], which can be a valid assumption when the battery state-of-charge (SOC) is below 80% charge [12]. Day-to-day operations require higher fidelity charging models to ensure buses have sufficient charge and to better incorporate the monitary cost of charging. In [8], [15], high-fidelity models are used at the price of requiring computationally intensive searches; [8] uses a genetic algorithm and [15] uses an exhaustive search strategy.

The contributions of this work include a Mixed-Integer Linear Program (MILP) scheduling framework that considers bus schedules, dynamics of the battery charging, limits on the state of charge, and a maximum number of available slow and fast chargers. This is, in part, made possible by focusing on the BEB charger scheduling, assuming that the charger locations and bus routes are fixed. Our formulation removes the always-on charging assumptions in prior work by solving for the charge interval lying within the total time window when buses visit the station. The optimal charging schedule defines the state of charge for each bus battery at each instant in time. This may be useful for building algorithms for real-time execution of charging schedules. The MILP problem is formed as a constrained network flow problem. Chargers are grouped by type and abstracted into a "flow" of slow and fast chargers, naturally allowing the number of chargers of each type to be a variable of optimization. A first-order dynamic model for charging is introduced to approximate the relationship between the time spent charging and the state of charge of the battery. This provides increased fidelity over a proportional model while fitting conveniently within a MILP framework. The cost of using a particular charger is allowed to vary throughout the day to account for time-varying power costs. The MILP framework also enables additional constraints to be introduced to respect the natural progression of each buses through the station. The solution of the problem provides the scheduling of when each bus should visit a slow or fast charger and, optionally, how many slow and fast charger are needed.

The remainder of the paper proceeds as follows. Preliminaries are presented in Section II. The scheduling problem for a single type of charger is described in Section III, with extensions to multiple types of chargers and optimizing over the number of chargers in Section IV. An example is then presented in Section V, showing the ability of the MILP framework to reduce charging costs, consider periods of high-

Email: {justin.whitaker greg.droge matthew.hansen daniel.mortensen jake.gunther}@usu.edu

Department of Electrical and Computer Engineering, Utah State University, Logan, UT 84322, USA.

cost charging, and determine the number of chargers needed. Section VI provides concluding remarks.

II. Preliminaries

A network is a directed graph whose edges (or arcs) have a defined capacity for moving some quantifiable element [16]. Nodes in the network are represented as vertices of the graph. Source nodes generate flow, sink nodes capture flow, and intermediary nodes serve as branching points for the flow. Network flow formulations have been used to describe a host of problems [17]. In this work, the network is used to determine the actions of chargers in a bus station.

The bus-charging network flow formulation depends upon two components. The first component is the underyling graph representing the network. Thus, graph fundamentals are presented in Section II-A, with the graph to be used described in Section II-B. The second component is the dynamic model of the battery charge, developed in Section II-C. Notation is summarized in Table I.

A. Graph Basics

A directed graph can be used to represent the network where the sources, sinks, and intermediary nodes are vertices of the graph and the arcs consist of directed edges in the graph. A graph G is defined as a set of vertices, V, and edges, $E \subset V \times V$, i.e. $G = \{V, E\}$. Given two vertices in the graph, $v_1, v_2 \in V$, an edge from v_1 to v_2 implies that the ordered pair (v_1, v_2) is in the edge set, i.e., $(v_1, v_2) \in E$. An example directed graph is shown in Fig. 1.

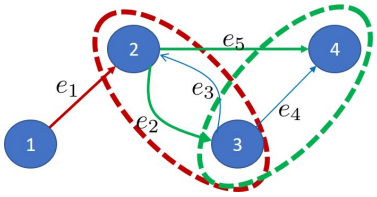

Fig. 1: Sample DAG where numbered circles show vertices and labeled arrows show directed edges. The colored ovals depict groups as discussed in Section III-B. Red and green edges correspond to the input edges of the groups.

As defined in [18], the incidence matrix can be used to represent the vertices and edges in matrix form and is denoted as D. Given $|V| = n_v$ and $|E| = n_e$, where $|\cdot|$ denotes the cardinality of a set, the incidence matrix is of dimension $n_v \times n_e$. Each column of D is used to represent an edge, while each row of D corresponds to a specific vertex. Using the notation $D = [d_{mn}]$ to denote the matrix such that the element in row m and column n is d_{mn}, the incidence matrix is defined as

$$D = [d_{mn}],\ d_{mn} = \begin{cases} 1 & \text{Edge } n \text{ begins at vertex } m \\ -1 & \text{Edge } n \text{ ends at vertex } m \\ 0 & \text{Otherwise} \end{cases}. \quad (1)$$

The incidence matrix of the graph in Fig. 1 can be written as

$$D = \begin{bmatrix} 1 & 0 & 0 & 0 & 0 \\ -1 & 1 & -1 & 0 & 1 \\ 0 & -1 & 1 & 1 & 0 \\ 0 & 0 & 0 & -1 & -1 \end{bmatrix}. \quad (2)$$

Edge indices are taken directly from the incidence matrix using the notation e_i to represent the edge corresponding to the i^{th} column of D. The edge index set, $\mathcal{I}$, is the set of integers from 1 to n_e.

B. Graph-based Representation of Charger Action Space

In this work, the network represents the flow of chargers from one task to another. Each vertex corresponds to a particular charger type either resting or charging a particular bus at a particular point in time. Integral to the concept of network flow is the idea that some quantity is moving ("flowing") from one node (vertex) to another along the edges. The edges in this scenario denote the possible transitions for the chargers. When at a rest vertex, a charger may transition to a subsequent rest vertex or it may transition to begin charging a bus. When at a charging vertex, a charger may transition to a subsequent charge vertex of the same bus, or it may transition to a rest vertex at the subsequent time. Due to route schedules, the buses are not always available to be charged and vertices for charging a bus are only present when the bus is available. An edge between an adjacent pair of charging vertices is present when the bus receives charge, i.e. no charge is given to a bus if the bus does not stay at the charger. A simplified example of such a graph is shown in Fig. 2.

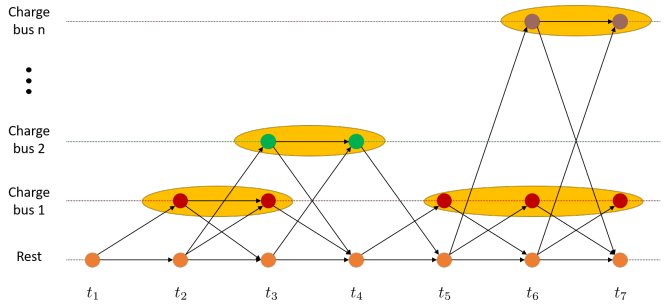

Fig. 2: A graph depicting the possible state and transitions for a single charger type over time for a very simple example. The bottom row corresponds to the charger at rest while the other rows each correspond to charging a particular bus. Yellow ovals are placed around charging windows.

Using the graph to represent possible actions of the charger, rather than possible actions for the bus, allows us to take advantage of the fact that the chargers are located at the same station. Instead of formulating a duplicate graph for each charger, all chargers of the same type and at the same station can be represented by the same graph in a network flow formulation, essentially leveraging the equivalence of all chargers to simplify the problem. Edges to charging vertices are restricted to allow only a unit flow; i.e., only one charger can charge bus i at a given time. A separate subgraph is used for each charger type to allow the edges to correspond to different charging rates and costs.

TABLE I: Notation used throughout the paper

Variable	Description	Variable	Description
Counters			
n_c	Number of charger types	n_{c_l}	Number of chargers of type l
n_b	Number of buses	n_v	Number of vertices
n_e	Number of edges	n_t	Number of time steps
n_g	Number of groups		
Indices			
i	Edge index	q	Vertex index
k	Time index	j	Bus index
l	Charger type index	p	Group index
m, n	General matrix indices		
Optimization Auxiliary Variables			
c_i	graph edge costs	c	Vector of edge costs c_i
Δ	The discretization time step	$\gamma_{j,k}$	Boolean indicating whether vertex for bus j at time k corresponds to a first slot time at the station
Charging variables			
M_j	Maximum charge of bus j	$\delta_{j,k}$	Discharge of bus j on route returning to station at time k
a_l	Charge rate of charger type l	$\bar{a}_l$	Discretized charge rate of charger type l
$\bar{b}_l$	Discretized charge offset of charger type l	$s_j(t)$	The continuous state-of-charge of bus j at time t
Graph variables			
G	A graph	V	A set of vertices
E	A set of edges	$\mathcal{I}$	The index set of edges
v_q	The q^{th} vertex	e_i	The i^{th} edge
D	Incidence matrix for the flow constraint	d_{mn}	Element in row m, column n of D
D_l	Incidence matrix for charger type l		
Decision and Slack variables			
$s_{j,k}$	State-of-charge of bus j at time k	s	Vector of charge variables $s_{j,k}$
$g_{j,k,l}$	Charge gain for bus j at time k from charger type l	g	Vector of gain variables $g_{j,k,l}$
x_i	Binary variable for using edge i	x	Vector of binary decision variables x_i
y	Concatenation of binary (x), charge (s), and gain (g) vectors		
Constraint variables			
b_{f_l}	Flow constraint rhs for charger type l	b_f	Stacked b_{f_l} for multiple-charger types flow constraint
$\mathbb{1}_m$	Vector of ones with m rows	$\mathcal{I}_p$	The index set of edges entering group p
A_g	The group constraint matrix	b_g	The group constraint rhs
A_{gain}^{jkl}	Charging dynamics constraint matrix for bus j at time k with charger type l	b_{gain}^{jkl}	Charging dynamics rhs
		$a_{m,n}^{jkl}$	Element m, n of A_{gain}^{jkl}
A_c^j	The charge constraint matrix of bus j	b_c^j	The charge constraint rhs
$a_{m,n}^{c\ j}$	Element m, n of A_c^j	A_{n_c}	Number of chargers constraint matrix
Index mappings			
$\sigma(j,k,l)$	Index of edge connecting the charging vertices for bus j between times $k-1$ and k using charger type l		
$\eta(j,k)$	Time index corresponding to final interval vertex before time k for bus j		
λ_v	The index of variable v to its index in y		

C. Dynamic Charging Model

Modelling the SOC of a battery can be complex as it depends upon both the chemistry of the battery and the charging algorithm to be employed. The battery model alone can vary based upon temperature, current, and cycling [19]. Care must be taken to balance the model accuracy with the ability to use the model within the optimization framework. A common battery charging control algorithm is CCCV [20], [21]: the charger applies a constant current (CC) to the battery until a battery terminal voltage is reached. The charger then holds that constant voltage (CV) as the charging current decreases. The charging current, which is approximately proportional to charge rate, is constant at low SOC and decreases as the SOC approaches full charge. We model this relationship using a first order differential system which, when given a step input, has a very similar exponential relationship between time and convergence to the maximum charge.

Index l is used to denote the l^{th} type of charger with a_l being the convergence rate of the charger. It is assumed that bus j has a battery with maximum charge M_j. Expressing the SOC of bus j at time step k as $s_{j,k}$, a discrete-time model is given in the following lemma.

Lemma 1. *Assume that the charge will occur over intervals of Δ seconds, the charge at time step $k+1$ for bus j can be related to the charge at time step k using charger l as*

$$s_{j,k+1} = \bar{a}_l s_{j,k} - \bar{b}_l M_j, \tag{3}$$

where

$$\bar{a}_l = e^{a_l \Delta},\ \bar{b}_l = e^{a_l \Delta} - 1.$$

Proof. A first-order, continuous model converging to M_j at an exponential rate of a_l can be expressed as

$$\dot{s}_j(t) = a_l s_j(t) - a_l M_j. \tag{4}$$

The resulting discrete model in (3) is obtained by using the exact discretization of an LTI system as in [22]. The exact discretization of a general LTI system, represented as $\dot{x}(t) = Ax(t) + Bu(t)$, with discretization time step Δ is given by (assuming $u(t)$ is held constant over the interval)

$$x_{k+1} = \bar{A}x_k + \bar{B}u_k,\ \bar{A} = e^{A\Delta},\ \bar{B} = \int_0^{\Delta} e^{A(\Delta-\tau)} d\tau B.$$

In (4), both a_l and M_l are constants and there is no actual control input. To utilize the general discretization formulation, we write (4) as $\dot{s}_j = a_l s_j(t) + b_l u(t)$ where $b_l = a_l$ and $u(t) = -M_l$. In terms of the general LTI formulation, the state $x(t)$ is replaced with $s_j(t)$ and the matrices A and B are replaced with a_l and b_l, respectively. Employing the discretization formula, the discretized forms of a_l and b_l become

$$\bar{a}_l = e^{a_l \Delta}, \; \bar{b}_l = \int_0^{\Delta} e^{a_l(\Delta - \tau)} d\tau.$$

The integral in $\bar{b}_l$ can be solved analytically by taking the anti-derivative as

$$\bar{b}_l = -\frac{1}{a_l} e^{a_l(\Delta-\tau)}|_{\tau=0}^{\tau=\Delta} = e^{a_l \Delta} - 1.$$

□

The charge of bus j will be calculated for each possible vertex that corresponds to charging bus j. While at the station, the charge will be represented using the piecewise dynamics

$$s_{j,k+1} = \begin{cases} \bar{a}_1 s_{j,k} - \bar{b}_1 M_j & \text{Using charger } 1 \\ \vdots & \vdots \\ \bar{a}_l s_{j,k} - \bar{b}_l M_j & \text{Using charger } l \\ s_{j,k} & \text{Not being charged} \end{cases}. \quad (5)$$

The update state can be expressed using a summation by introducing the variables $g_{j,k,l}$ as the gain in battery charge for bus j at time step k from charger type l. The gain can be expressed piecewise as

$$g_{j,k,l} = \begin{cases} (\bar{a}_l - 1) s_{j,k} - \bar{b}_l M_j & \text{Using charger } l \\ 0 & \text{otherwise} \end{cases}. \quad (6)$$

Denoting n_c as the number of charger types, the charge while at the station can be expressed as

$$s_{j,k+1} = s_{j,k} + \sum_{l=1}^{n_c} g_{j,k,l}. \quad (7)$$

The amount of charge required for bus j to execute its route and return to the station at time k is denoted as $\delta_{j,k}$. Given that the bus re-enters the station at time k, the mapping $\eta(j,k)$ is used to denote the previous time index that bus j was in the station prior to time k. The dynamics across this interval can then be written as

$$s_{j,k} = s_{j,\eta(j,k)} - \delta_{j,k}. \quad (8)$$

III. Network Flow Bus Scheduling Formulation for a Single Charger Type

This section progressively builds to the electric bus charging problem for a single type of charger. A MILP is first presented for the pure network flow problem. This forms the fundamental ability to plan for multiple chargers of the same type. The solution to the MILP determines which edges in the graph will be used as well as the number of chargers that will take a given edge. Constraints on the flow into vertex groups are then introduced to ensure that at most one charger will be assigned to a bus each time it visits the station. The final portion of this section introduces variables and constraints to track the dynamics of each bus charge and constrain the lower limit of the charge.

A. A Network Flow Approach to Graph Search

This section presents a MILP formulation of the graph search problem that allows for simultaneous search of multiple routes through the graph. An integer decision variable is introduced for each edge in the graph, denoted as x_i for $i \in \mathcal{I}$ (recall that $\mathcal{I}$ is the index set over the edges). A value $x_i > 0$ indicates that edge i is selected as part of the flow from the start to the goal. A value of 0 indicates that it is not selected. To select one path over another, a value is assigned to each edge, denoted as c_i. As a minimization problem will be formulated, $c_i > 0$ denotes an edge cost or penalty. The total cost of a selected path can be written as the summation of the incurred costs, $c_1 x_1 + c_2 x_2 + ... + c_{n_e} x_{n_e}$. This can be written more succinctly as $c^T x$, where both c and x are column vectors.

Constraints must be introduced to balance the flow through the network so that the chosen path moves continuously from one vertex to another through the graph. The starting vertices are sources with positive flow, the ending are sinks with negative flow, and all others must have the same outgoing flow as incoming flow. This balance of flow can be represented as a constraint using the incidence matrix. Recall that the edge directionality is encoded into the incidence matrix. Summing across row q of D will give the number of edges originating at vertex v_q minus the number of edges ending at vertex v_q. As x represents the amount of flow along each edge, Dx is a column vector where each row corresponds to the outgoing flow minus the incoming flow for the vertex.

Assuming that a single source vertex (i.e., all chargers start at "rest") is the first vertex and that a single sink vertex (i.e., all chargers end at "rest") is the final vertex, the network flow constraint assuming a single type of charger ($l = 1$) can be written as

$$Dx = b_{f_1}, \; b_{f1} = \begin{bmatrix} n_{c_1} & 0 & ... & 0 & -n_{c_1} \end{bmatrix}^T, \quad (9)$$

where n_{c_l} is the number of chargers of type l. The optimization problem can then be re-written to include this constraint as

$$\begin{aligned} &\min_x \; c^T x \\ &\text{s.t. } Dx = b_{f_1}, \; x_i \in \{0, ..., n_{c_l}\} \end{aligned}. \quad (10)$$

Note that (10) is very similar to the formulation in Chapter 10 of [17], using different notation and expressing the constraint in matrix form using the incidence matrix.

A simple network flow example: Consider the simple example from (2) depicted in Fig. 1. Assuming a source flow of 1, the network flow constraint in (9) can be reduced to

$$Dx = \begin{bmatrix} x_1 \\ -x_1 + x_2 - x_3 + x_5 \\ -x_2 + x_3 + x_4 \\ -x_4 - x_5 \end{bmatrix} = \begin{bmatrix} 1 \\ 0 \\ 0 \\ -1 \end{bmatrix}.$$

A row-by-row overview of the constraint can help to understand the flow constraint. Row 1 indicates that e_1 must be used. This is also obvious from Fig. 1 as it is the only edge

coming out of the source vertex. Row four states that either e_4 or e_5 be selected, but not both due to constraint that x_i be non-negative integers. Rows two and three show the balance of incoming and outgoing edges.

B. Group Constraints

One significant advantage of using the MILP formulation for performing a graph search is the ability to add additional constraints. One constraint of import is that during each stop at the station, a bus may visit at most one charger, with an optional wait before and after charging, as needed. Given a group of vertices corresponding to a single visit, a constraint can be introduced to limit the aggregate input and output flow of that group of vertices. In what follows, solely the input constraints are considered. Given a constraint on the input flow, the balancing property of the network flow constraint will enforce that the output flow be constrained to the same value if the group does not contain a source vertex.

Denote vertex group p as $\mathcal{V}_p \subset V$ with the index set of the edges leading into group p defined as

$$\mathcal{I}_p = \{i | e_i \in E \text{ where } e_i = (v_m, v_n), \\ v_m \in \mathcal{V}_p, \text{ and } v_n \in V \setminus \mathcal{V}_p\} .$$

The constraint that a bus be charged by only a single charger when at the station can be written in summation form as

$$\sum_{i \in \mathcal{I}_p} x_i \leq 1,\ p = 1, ..., n_g,$$

where n_g is the number of groups. Combined with the constraint that x_i is integer ensures that either zero or one edge will come into and out of group p.

The definition of $\mathcal{I}_p$ can be used to write the constraint in matrix form to be more amenable to optimization routines. The matrix A_g and vector b_g are used to represent the constraint as $A_g x \leq b_g$, $b_g = \mathbb{1}_{n_g}$, where $\mathbb{1}_m$ is a column vector of m ones. Allowing a^g_{mn} to be the entry of A_g in the m^{th} row and n^{th} column, A_g can be expressed as

$$A_g = [a^g_{mn}],\ a^g_{mn} = \begin{cases} 1 & n \in \mathcal{I}_m \\ 0 & \text{otherwise} \end{cases} .$$

The optimization problem for a single type of charger with group constraints can be written as

$$\min_x\ c^T x \\ \text{s.t. } Dx = b_{f_1},\ A_g x \leq b_g,\ x_i \in \{0...n_{c_1}\} . \tag{11}$$

Continuing the Simple Example: The groups shown in Fig. 1 are now evaluated. The red vertex group is formed with vertices v_2 and v_3 and the green is formed with vertices v_3 and v_4. The edge index sets can be written as $\mathcal{I}_1 = \{1\}$ and $\mathcal{I}_2 = \{2, 5\}$. The summation and matrix forms of the constraints can be written as

$$\begin{matrix} x_1 \leq 1 \\ x_2 + x_5 \leq 1 \end{matrix} \text{ or } \begin{bmatrix} 1 & 0 & 0 & 0 & 0 \\ 0 & 1 & 0 & 0 & 1 \end{bmatrix} x \leq \begin{bmatrix} 1 \\ 1 \end{bmatrix} .$$

C. Charging Variables and Constraints

Each edge in the graph corresponds to a charger resting, transitioning to or from charging, or charging a particular bus. Recall from Section II-C that the variable $g_{j,k,l}$ is the gain for bus j using an edge starting at time k on charger type l. The mapping $\sigma(j,k,l)$ is used to map to the respective edge index, i.e., $x_{\sigma(j,k,l)}$ is the flow associated with the same edge as gain $g_{j,k,l}$. As only a single charger type is available in this section, the value $l = 1$ is used.

The case statement for the gain in (6) can be represented as an either/or constraint. Using Big-M notation, the case statement in (6) can be represented as

$$\begin{matrix} g_{j,k,l} \geq (\bar{a}_l - 1)s_{j,k} - \bar{b}_l M_j - M_j(1 - x_{\sigma(j,k,l)}) \\ g_{j,k,l} \leq (\bar{a}_l - 1)s_{j,k} - \bar{b}_l M_j \\ g_{j,k,l} \geq 0 \\ g_{j,k,l} \leq 0 + M_j x_{\sigma(j,k,l)} \end{matrix} , \tag{12}$$

where the Big-M components are expressed in blue and $l = 1$. Note that when edge $x_{\sigma(j,k,l)}$ is used (i.e., equals 1 due to the group constraint) then the top two equations will form the appropriate equality constraint for charging and the fourth equation will allow the charge gain to extend up to the maximum charge. When $x_{\sigma(j,k,l)} = 0$ then the final two equations are active, forcing the gain to be zero while the first equation will allow the gain to extend down to zero. Note that (12) can be written in a standard linear constraint form as

$$\begin{matrix} (\bar{a}_l - 1)s_{j,k} + M_i x_{\sigma(j,k,l)} - g_{j,k,l} \leq M_j(\bar{b}_l + 1) \\ g_{j,k,l} - (\bar{a}_l - 1)s_{j,k} \leq -\bar{b}_l M_j \\ -g_{j,k,l} \leq 0 \\ g_{j,k,l} - M_j x_{\sigma(j,k,l)} \leq 0 \end{matrix} . \tag{13}$$

This can be expressed in matrix form. Denote the variables of optimization as

$$y = \begin{bmatrix} x & \text{All edge variables} \\ s & \text{All charge variables} \\ g & \text{All gain variables} \end{bmatrix} .$$

The mapping λ_v is used to represent the index of variable v in y. The constraints in (13) will be repeated for every possible j, k, l combination (i.e. for each time k when charging is possible for bus j and for each charger type, l). This four-row matrix is denoted as A^{jkl}_{gain} with the constraint written as $A^{jkl}_{gain} y = b^{jkl}_{gain}$. Defining A^{jkl}_{gain} elementwise as

$A^{jkl}_{gain} = [a^{jkl}_{mn}]$, the elements can be expressed as

$$a^{jkl}_{1n} = \begin{cases} (\bar{a}_l - 1) & n = \lambda_{s_{j,k}} \\ M_j & n = \lambda_{x_{\sigma(j,k,l)}} \\ -1 & n = \lambda_{g_{j,k,l}} \\ 0 & \text{otherwise} \end{cases}$$

$$a^{jkl}_{2n} = \begin{cases} -(\bar{a}_l - 1) & n = \lambda_{s_{j,k}} \\ 1 & n = \lambda_{g_{j,k,l}} \\ 0 & \text{otherwise} \end{cases} \quad b^{jkl}_{gain} = \begin{bmatrix} M_j(\bar{b}_l + 1) \\ -\bar{b}_l M_j \\ 0 \\ 0 \end{bmatrix}$$

$$a^{jkl}_{3n} = \begin{cases} -1 & n = \lambda_{g_{j,k,l}} \\ 0 & \text{otherwise} \end{cases}$$

$$a^{jkl}_{4n} = \begin{cases} 1 & n = \lambda_{g_{j,k,l}} \\ -M_j & n = \lambda_{x_{\sigma(j,k,l)}} \\ 0 & \text{otherwise} \end{cases}$$

The aggregate charging inequality constraint $A^{ineq}_{gain} y \leq b^{ineq}_{gain}$ is defined by stacking A^{ikl}_{gain} and b^{ikl}_{gain} for $i = 1, ..., n_b$, for all k such that a charging vertex is available for bus j and for each charger type l.

With the edge charge gains in hand, the charger updates in (7) and (8) can be expressed. They take the form of an equality constraint, one for each bus and time that a charging vertex appears. Recall that (8) models the change in charge after a bus has run its route and (7) models the charge while at the station. Thus, the first vertex in each group of charging vertices will use (8) and the rest will use (7). The boolean $\gamma_{j,k}$ is used to indicate starting vertices of groups, defined as

$$\gamma_{j,k} = \begin{cases} 1 & k \text{ is the time of a first group vertex for bus } j \\ 0 & \text{otherwise} \end{cases}.$$

The equality constraint corresponding to bus j can be expressed as $A^j_c y = b^j_c$ where

$$A^j_c = [a^{c,j}_{k,n}] = \begin{cases} 1 & n = \lambda_{s_{j,k}} \\ 1 & \exists\ l \text{ s.t. } n = \lambda_{g_{j,k,l}} \\ -1 & n = \lambda_{s_{j,k+1}} \text{ and } \gamma_{j,k} = 0 \\ -1 & n = \lambda_{s_{j,\eta(j,k)}} \text{ and } \gamma_{j,k} = 1 \\ 0 & \text{otherwise} \end{cases}.$$

$$b^j_c = [b^{c,j}_k] = \begin{cases} s_{j,1} & k = 1 \\ -\delta_{j,k} & \gamma_{j,k} = 1 \\ 0 & \text{otherwise} \end{cases}$$

The full equality constraint, $A^{eq}_c y = b^{eq}_c$, is formed by stacking A^j_c and b^j_c for $j = 1, ...n_b$.

The full optimization problem can be expressed as

$$\begin{gathered} \min_y\ c^T y \\ \text{s.t. } Dx = b_{f_1},\ A_g x \leq b_g \\ A^{ineq}_c y \leq b^{ineq}_c,\ A^{eq}_c y = b^{eq}_c, \\ x_i \in \{0...n_{c_1}\},\ s_{j,k} \geq s_{j,min} \\ y = [x^T, d^T, g^T]^T \end{gathered} \tag{14}$$

where $s_{j,min}$ is the minimum charge allowed. The objective term c could be designed to penalize charging edges and/or charge values.

IV. Extensions for Multiple Charger Types and Numbers of Chargers

The optimization problem presented in the previous section considered a single charger type with a fixed number of chargers. These two assumptions will be relaxed in the following developments.

A. Multiple Charger Types

Consider the scenario of a station with multiple types of chargers, each type having a potentially different charging rate, cost of usage, and quantity. As before, when a bus arrives to the station it can only visit a single charger prior to departing. The optimization must now include the ability to select which type of charger is used. Changes in the flow constraint, the group constraint, and the charge constraint are now addressed.

1) Updated Flow Constraint: A separate graph of charging availability can be designed for each charger type. Given n_c different types of chargers, the aggregate charging graph would be a set of disjoint subgraphs. Each subgraph would have a defined starting and end vertex with the l^{th} charger type incidence matrix being denoted as D_l. The aggregate incidence matrix would be the block diagonal matrix

$$D = \begin{bmatrix} D_1 & 0 & ... & 0 \\ 0 & \ddots & \ddots & \vdots \\ \vdots & \ddots & \ddots & 0 \\ 0 & ... & 0 & D_{n_c} \end{bmatrix}.$$

The right-hand side of the flow constraint can be formed by stacking b_{f_l} for $l = 1, ..., n_c$ as

$$b_f = \begin{bmatrix} b^T_{f_1} & ... & b^T_{f_{n_c}} \end{bmatrix}^T.$$

The flow constraint is defined similar to before as $Dx = b_f$.

2) Updated Group Constraint: The form of the group constraint does not change, only that vertices in a group will now span the disjoint sub-graphs for each charger type. As before, a group consists of a set of vertices $\mathcal{V}_p$ defined by all of the vertices corresponding to a particular visit by a bus to the station. The set $\mathcal{V}_p$ now contains the vertices across the various disjoint graphs that correspond to a particular visit by the bus to the station.

3) Updated Charging Constraint: Under a single type of charger, the summation in (7) included a single gain term. Under multiple types of chargers, the summation will include n_c terms. For homogeneous charger schedules, there will be n_c slack variable gains added for each possible charging edge. The charge constraint takes the same form as before with $l = 1, ..., n_c$ instead of $l = 1$.

B. Optimizing the Number of Chargers

To choose the number of chargers, the variables of optimization are augmented with n_c additional variables as

$$y = \begin{bmatrix} x & \text{All edge variables} \\ s & \text{All charge variables} \\ g & \text{All gain variables} \\ [n_{c_1}\ ...\ n_{c_{n_c}}]^T & \text{Number of chargers of each type} \end{bmatrix}.$$

The group and charge constraints are zero padded by adding an additional n_c columns of zeros to the A_g and A_c matrices. The flow constraint is updated to $\begin{bmatrix} D & 0 & A_{n_c} \end{bmatrix} y = 0$, where the 0 on the left-hand side accounts for no inclusion of s and g in the constraint and the 0 on the right-hand side is a column vector. The additional A_{n_c} matrix is an $n_v \times n_c$ matrix defined as the block diagonal

$$A_{n_c} = \begin{bmatrix} -b_{f_1} & 0 & ... & 0 \\ 0 & \ddots & \ddots & \vdots \\ \vdots & \ddots & \ddots & 0 \\ 0 & ... & 0 & -b_{f_{n_c}} \end{bmatrix}.$$

V. Example

An example is now presented to illustrate the utility of the developed planning techniques. A description of the station scenario is first presented followed by the description of the strategies used for planning. Results are then presented for three separate optimization scenarios where the planning strategies are employed.

A. Battery Electric Bus station Scenario

The bus station is required to charge 30 battery electric buses using a combination of slow and fast battery chargers. Each bus is equipped with a 388 KWh battery that is required to stay above 25% charge (97 kWh) to maintain battery health. Planning occurs over a 24 hour period where each bus is assumed to start with 90% charge (349.2 kWh). To enable repeatability in the charging scheme the next day, each bus is required to also end with at least 90% charge. Slow, low-cost charging can take several hours while fast, high-cost charging can be a fraction of an hour [4]. Thus, the low-cost charger is modeled with a value of $a_1 = 0.01$, which would charge a battery from zero charge to 90% charge in a little under four hours. The high-cost charger is modeled with a value of $a_2 = 0.1$, resulting in a 90% charge in 23 minutes. While the high-cost charger is ten times faster, it is modeled as being twenty times as expensive per hour, i.e. twice the cost to obtain the same charge. This is to model both the higher cost of energy usage and to penalize the increased wear on the battery resulting from fast charging.

The bus schedules are randomly generated. It is assumed that each bus route will take between 50 and 180 minutes to execute. Buses will then return to the station for a duration between 60 and 120 minutes before leaving again and are assumed to be in the station for at least 120 minutes at the end of the 24 hour period. To calculate the amount of discharge along the route (i.e., $\delta_{j,k}$), it is assumed that the buses use 30 kWh of charge every hour while in route.

The planning occurs for a single 24 hour period at a ten minute resolution. The resulting randomly generated buses produce a total of 4,744 vertices, 13,248 edges, and 6,338 total charging slack variables. The optimization is performed using the Gurobi MILP solver [23] on a machine running a quad-core Intel i7-8650U 1.9 GHz processor. Note that even with 30 slow chargers (i.e., one per bus – charging the buses at every opporunity), the requirement that each bus ends with at least 90% charge cannot be met. This necessitates the use of both slow and fast chargers.

B. Planning Strategies

Three separate planning strategies are employed:
Naive: Buses are assigned to chargers as they come into the station, prioritized by their current charge level.
No-Zone: The MILP formulation is used with a cost of 1 assigned to each edge corresponding to charging at a slow charger and a cost of 20 for edges corresponding to charging at a fast charger. Transition and rest edges are assigned zero cost.
Zone: The MILP formulation is used with edge costs assigned as in the *No-Zone* strategy except for the addition of two periods (or "zones") of time in which the cost of charging is much higher, emulating periods with high peak demand. During these periods of high-demand, the edge cost for charging with a slow charger increases to 50 and those corresponding to a fast charger increase to 100.

The *Naive* approach prioritizes assignment of available buses to chargers based upon the battery level of the buses to emulate a clerk making assignments as buses enter the station. It is similar to the thresholding strategy discussed in [15], albeit with multiple thresholds to account for various charger types and without the exhaustive search for the best thresholds. It employs a rule-based system for assigning buses. Three different charging thresholds are given: low charge (60%), medium charge (75%) and high charge (90%). Buses below a low charge are prioritized to a fast charger if available, and a slow charger otherwise. The next priority comes to buses that are above low but below medium. These are assigned first to a slow charger if available and second to a fast charger. Buses below the high threshold and above the medium threshold are then prioritized to a slow charger if available, never being assigned to a fast charger. Buses above the high-charge level are not assigned to a charger. Once assigned a charger, the bus stays on the charger until its battery reaches 90% charge or it is time to begin its next route, whichever comes first. The main benefit of the naive approach is that the full 24 hour period can be planned in less than a second.

C. Scheduling Scenarios

Three scheduling scenarios are now considered and results discussed. The first is a scenario in which an excess of chargers exist, the second scenario considers the minimization of chargers, and the third scenario considered planning with the reduced number of chargers. The results are plotted in Figs. 3 to 5. Figures 3 and 4 plot the aggregate mean, max, and min charge for each strategy as well as the charger utilization over time. The zones of high-cost charging are shaded pink. Figure 5 shows two example charge profiles for the buses under two planning strategies. Table II compares the resulting solutions in a number of ways. The mean expresses the level of charge that was nominally maintained. The *Min Charge* and *Min Final Charge* columns show whether the minimum constraints are met over all time and at the final time, respectively. The starting and ending optimality gap give

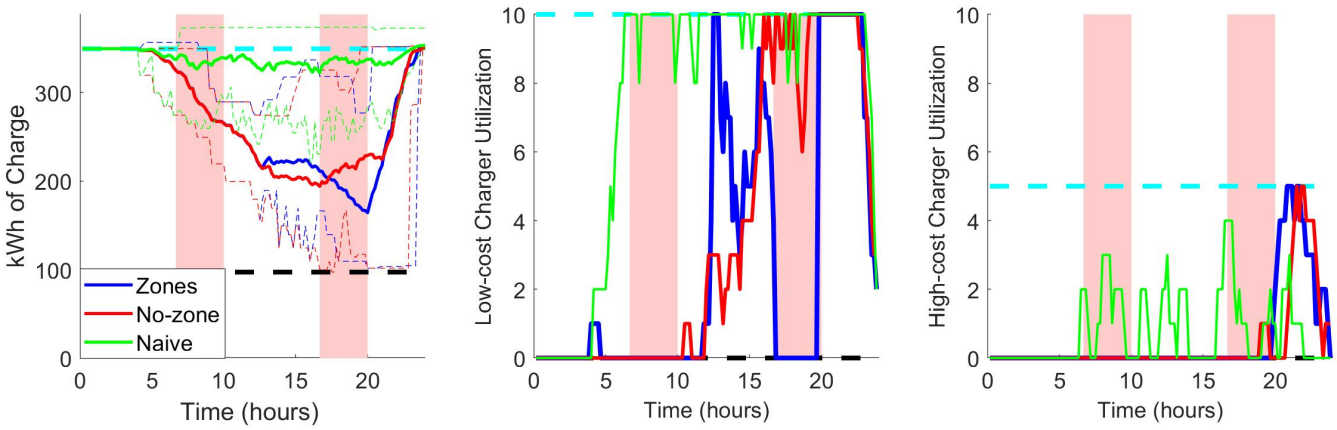

Fig. 3: Aggregate results for ten low-cost chargers and five high-cost chargers. Blue uses MILP considering high-cost time zones, red uses MILP without considering high cost, and green represents using the naive approach. Left shows the mean charge (solid) as well as max an min charge (dotted) over time. The middle shows the low-cost charger utilization and the right shows the high-cost charger utilization.

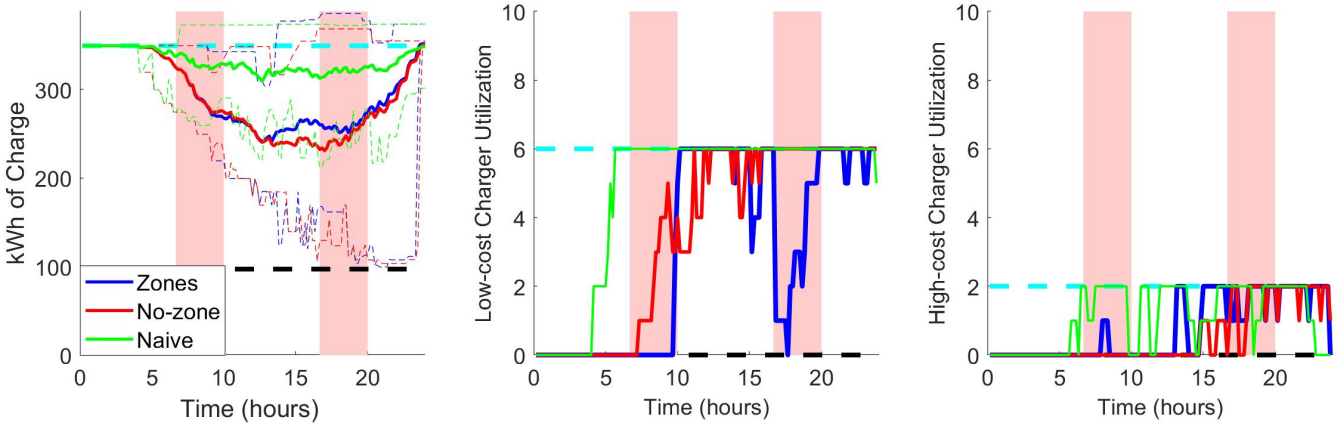

Fig. 4: Aggregate results for six low-cost chargers and two high-cost chargers. Blue uses MILP considering high-cost time zones, red uses MILP without considering high cost, and green represents using the naive approach. Left shows the mean charge (solid) as well as max an min charge (dotted) over time. The middle shows the low-cost charger utilization and the right shows the high-cost charger utilization.

the level of improvement in the MILP solutions in the time allotted. Recall that the "Zones" and "No Zones" strategies use different weightings during optimization. To show the benefit of considering the zones of high-cost time, the resulting cost calculated with both weightings for each solution is shown in Table II under the column headings *Cost Zones* and *Cost No Zones*. The final two columns of the table show the cumulative amount of time that each charger type was used by all buses over the 24 hour period.

Excess Chargers: This scenario assumes that a fixed number of chargers is available. A total of ten slow chargers and five fast chargers are used. The *Naive* strategy was used as a warm start to the MILP optimization so show the improvement of the MILP solution over the naive solution[1]. The MILP optimizations were allowed to run for thirty minutes.

[1]Note that even without the warm start, the MILP solver is able to find a better solution than the *Naive* approach after five minutes.

The *Naive* strategy is nearly able to meet charging thresholds, albeit with a significant cost and utilization of the chargers. Table II shows that the resulting cost of the *Naive* approach is twice that of the MILP solution when high-cost zones are not considered and nearly twenty times the cost when high-cost zones are considered. In contrast, MILP is able to adapt to different circumstances. The *Zone* strategy is able to reduce the cost by nearly 90% over the *No-Zone* strategy by avoiding high-cost zones. The resulting solution from the *Zone* strategy has less than a 10% increase in cost when the zones are not considered. Figure 3 shows that for the *Zones* strategy to meet charge requirements without charging during high-cost times, the mean charge is ramped up slightly before entering the second costly charge zone. A comparison of the *Zones* and *No-Zones* MILP strategy results show that excess number of chargers can be used to avoid costly time windows. The *Zones* strategy uses zero chargers during the high-cost time windows, greatly reducing the resulting cost.

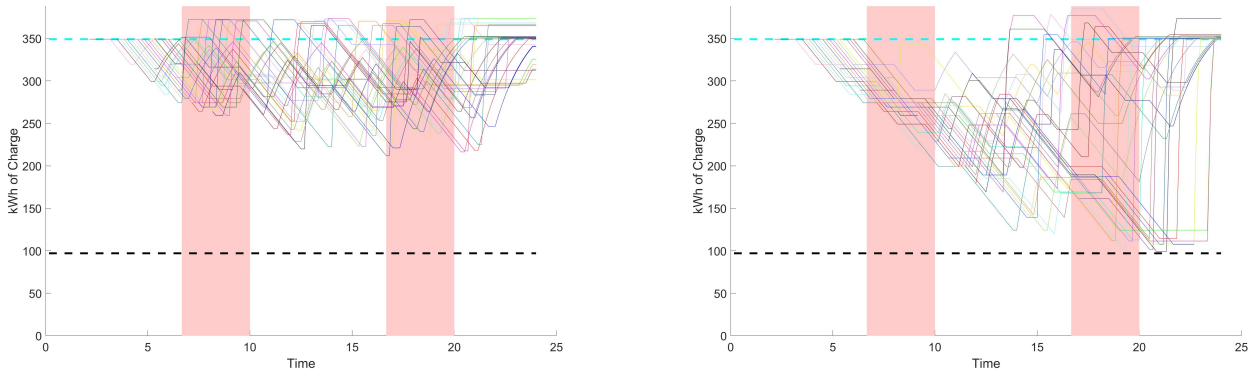

Fig. 5: Shows the charge vs time for each bus using the *Naive* strategy (left) and the *Zones* strategy (right) for the *Reduced Chargers* scenario where 6 slow and 2 fast chargers are used.

TABLE II: The first column describes the configuration of the strategy used to find a solution. The numbers correspond to the number of fast and slow chargers, *Zones* indicates the weightings used for optimization considering high-cost zones, and *No Zones* indicates that the high cost zones did not receive higher weightings, *Naive* is the threshold strategy, and *Num Chargers* is optimizing over the number of chargers. Columns 2 and 3 are the mean and minimum charge of all buses over time, Column 4 is the minimum charge of any bus at the final time. Columns 5 and 6 are the starting and ending optimality gap output by Gurobi. Columns 7 and 8 are the cost of the solution calculated with and without the higher zone rates. Columns 9 and 10 are the total minutes that a slow and fast charger were used.

Configuration	Mean Charge (kWh)	Min Charge (kWh)	Min Final Charge (kWh)	Start Gap	End Gap	Cost Zones	Cost No Zones	Slow Charger Utilization (Minutes)	Fast Charger Utilization (Minutes)
10-5 Zones	273	101	349.2	96.4%	42.3%	1,083	1,083	3,950	760
10-5 No-Zones	275	97	349.2	83.1%	47.9%	8,299	985	5,140	580
10-5 Naive	339	221	348	–	–	19,366	1,887	10,760	1,080
Num Chargers	292	99	349.2	100%	57.5%	–	–	4,610	960
6-2 Zones	295	99	349.2	93.5%	85.4%	4,827	1,440	4,320	1,090
6-2 No-Zones	290	101	349.2	72.1%	53.5%	8,354	1,189	5,110	810
6-2 Naive	331	211	301.4	–	–	13,592	2,016	6,830	1,570

Table II shows that to avoid the costly windows, the amount of time spent on the fast chargers is increased by over 30%.

Using the MILP strategies, the mean and minimum battery charge values are allowed to dip much lower than the Naive strategy while the max charge rarely exceeds the requisite end charge. Thus, less time is spent on unneeded charging. The *Naive* strategy uses the chargers for a much larger amount of time while still not quite meeting the terminal charge requirement. While the MILP solutions use the fast charger for far less aggregate time than the *Naive* strateigy, they use it significantly more in the final hours of the day. By allowing the battery charge to dip low, the MILP solutions are able to capitalize on the increased charge received per unit time at lower charge levels.

Charger Minimization: Facility constraints may limit the number of chargers in a single station. The formulation in Section IV-B can be used to determine the number of required chargers. To determine the minimum number of chargers needed to satisfy requirements, all weights can be zeroed except for the weights on the number of chargers of each type. In this example, the fast charger was assigned a cost of ten times that of the slow charger to emulate the higher initial and operational costs of fast charging. Furthermore, as the possible space is constrained, the number of chargers were limited to a maximum of ten low-cost chargers and five high-cost chargers.

Optimizing over the number of chargers significantly slowed down the optimization time. While a feasible solution was rapidly found, the optimization took nearly six hours to reduce the chargers to six slow and two fast with a resulting optimality gap of 58.6%. After six additional hours, the number of chargers did not change and the optimality gap had decreased to only 57.5%. Note that this optimization duration is not prohibitive, as the question of how many chargers to install will likely not be asked on a daily basis.

Reduced Chargers: Using the number of chargers found in the *Charger Minimization* scenario, the three planning strategies were again employed with results shown in Figs. 4 and 5 and Table II. The MILP strategies used the solution of the *Charger Minimization* as a warm start and optimized for another thirty minutes with the number of chargers fixed. While the *Naive* approach appears to not perform too much worse when examining the costs in Table II, it does not meet the final charge constraints. This is readily apparent in Fig. 5 where several buses end below the final charge threshold. The MILP is again able to adjust to have a lower cost when considering the zones of high-cost time, but there is less flexibility than with more chargers. The *Zones* strategy still utilizes chargers during zones of high cost, although it does use less chargers during high-cost regions than the *No-Zones* strategy. Similar to the *Excess Chargers* scenario, Table II

shows that the *Zones* strategy again appears to ramp up the mean charge prior to the second zone of high cost and uses the fast chargers for more time than the *No-Zones* strategy.

VI. Conclusion

This work developed a scheduling framework to balance the use of slow and fast chargers assuming the bus routes and charger locations were fixed. A DAG was used to model the available charge times for buses that routinely visit a station for charging. The incidence matrix of the DAG was used to formulate a network flow constraint, group constraints were used to enforce the natural progression of the bus through the station at each visit, and charging constraints were added to model the battery charge of each bus using a first-order dynamic model. A MILP problem was formulated to enable the scheduling of BEB charging as well as determine the required number of chargers.

An example was presented that demonstrated the the ability of the MILP formulation to utilize slow chargers when possible and fast chargers when needed to accommodate timing constraints and ensure a sufficient charge for route execution. The optimization was performed under three different scenarios. An excess of chargers existed in the first scenario and the scheduling framework was able to use the excess chargers to completely avoid times of high cost. The second scenario demonstrated the ability of the scheduling framework to reduce the number of chargers required. With this reduced number of chargers, the third scenario again optimized over the schedule. While not completely able to avoid high-cost periods, the scheduling framework was still able to significantly reduce costs while meeting charging threshold requirements. In each scenario the slow chargers were used significantly more than the fast chargers with increased fast charger usage when peak-time costs needed to be avoided.

Acknowledgment

This material is based in part upon work supported by the National Science Foundation through the ASPIRE Engineering Research Center under Grant No. EEC-1941524, the Department of Energy through a prime award with ABB under Grant No. DE-EE0009194, and PacifiCorp under contract number 3590. Any opinions, findings, and conclusions or recommendations expressed in this material are those of the authors and do not necessarily reflect the views of the National Science Foundation, the Department of Energy, or Pacificorp.

References

[1] G. De Filippo, V. Marano, and R. Sioshansi, "Simulation of an electric transportation system at The Ohio State University," *Applied Energy*, vol. 113, pp. 1686–1691, 2014.

[2] M. Xylia and S. Silveira, "The role of charging technologies in upscaling the use of electric buses in public transport: Experiences from demonstration projects," *Transportation Research Part A: Policy and Practice*, vol. 118, pp. 399–415, 2018.

[3] U. Guida and A. Abdulah, "ZeEUS eBus Report #2 - An updated overview of electric buses in Europe," International Association of Public Transport (UITP), Tech. Rep. 2, 2017. [Online]. Available: http://zeeus.eu/uploads/publications/documents/zeeus-ebus-report-2.pdf

[4] J.-Q. Li, "Battery-electric transit bus developments and operations: A review," *International Journal of Sustainable Transportation*, vol. 10, no. 3, pp. 157–169, 2016.

[5] N. Lutsey and M. Nicholas, "Update on electric vehicle costs in the United States through 2030," *The International Council on Clean Transportation*, vol. 2, 2019.

[6] S. N. Motapon, E. Lachance, L. A. Dessaint, and K. Al-Haddad, "A generic cycle life model for lithium-ion batteries based on fatigue theory and equivalent cycle counting," *IEEE Open Journal of the Industrial Electronics Society*, vol. 1, pp. 207–217, 2020.

[7] R. Wei, X. Liu, Y. Ou, and S. K. Fayyaz, "Optimizing the spatio-temporal deployment of battery electric bus system," *Journal of Transport Geography*, vol. 68, pp. 160–168, 2018.

[8] M. T. Sebastiani, R. Lüders, and K. V. O. Fonseca, "Evaluating electric bus operation for a real-world BRT public transportation using simulation optimization," *IEEE Transactions on Intelligent Transportation Systems*, vol. 17, no. 10, pp. 2777–2786, 2016.

[9] A. Hoke, A. Brissette, K. Smith, A. Pratt, and D. Maksimovic, "Accounting for lithium-ion battery degradation in electric vehicle charging optimization," *IEEE Journal of Emerging and Selected Topics in Power Electronics*, vol. 2, no. 3, pp. 691–700, 2014.

[10] Y. Wang, Y. Huang, J. Xu, and N. Barclay, "Optimal recharging scheduling for urban electric buses: A case study in Davis," *Transportation Research Part E: Logistics and Transportation Review*, vol. 100, pp. 115–132, 2017. [Online]. Available: https://www.sciencedirect.com/science/article/pii/S1366554516305725

[11] Y. Zhou, X. C. Liu, R. Wei, and A. Golub, "Bi-objective optimization for battery electric bus deployment considering cost and environmental equity," *IEEE Transactions on Intelligent Transportation Systems*, vol. 22, no. 4, pp. 2487–2497, 2020.

[12] T. Liu and A. (Avi) Ceder, "Battery-electric transit vehicle scheduling with optimal number of stationary chargers," *Transportation Research Part C: Emerging Technologies*, vol. 114, pp. 118–139, 2020. [Online]. Available: https://www.sciencedirect.com/science/article/pii/S0968090X19304061

[13] C. Yang, W. Lou, J. Yao, and S. Xie, "On charging scheduling optimization for a wirelessly charged electric bus system," *IEEE Transactions on Intelligent Transportation Systems*, vol. 19, no. 6, pp. 1814–1826, 2018.

[14] X. Wang, C. Yuen, N. U. Hassan, N. An, and W. Wu, "Electric vehicle charging station placement for urban public bus systems," *IEEE Transactions on Intelligent Transportation Systems*, vol. 18, no. 1, pp. 128–139, 2017.

[15] N. Qin, A. Gusrialdi, R. Paul Brooker, and A. T-Raissi, "Numerical analysis of electric bus fast charging strategies for demand charge reduction," *Transportation Research Part A: Policy and Practice*, vol. 94, pp. 386–396, 2016. [Online]. Available: https://www.sciencedirect.com/science/article/pii/S096585641630444X

[16] R. Burkard, M. Dell'Amico, and S. Martello, *Assignment problems: revised reprint*. SIAM, 2012.

[17] D.-S. Chen, R. G. Batson, and Y. Dang, *Applied integer programming*. Wiley, 2010.

[18] M. Mesbahi and M. Egerstedt, *Graph theoretic methods in multiagent networks*. Princeton Univ Pr, 2010.

[19] N. Watrin, R. Roche, H. Ostermann, B. Blunier, and A. Miraoui, "Multiphysical lithium-based battery model for use in state-of-charge determination," *IEEE Transactions on Vehicular Technology*, vol. 61, no. 8, pp. 3420–3429, 2012.

[20] L.-R. Chen, R. C. Hsu, and C.-S. Liu, "A design of a grey-predicted Li-ion battery charge system," *IEEE Transactions on Industrial Electronics*, vol. 55, no. 10, pp. 3692–3701, 2008.

[21] A. Abdollahi, X. Han, G. Avvari, N. Raghunathan, B. Balasingam, K. Pattipati, and Y. Bar-Shalom, "Optimal battery charging, part I: Minimizing time-to-charge, energy loss, and temperature rise for OCV-resistance battery model," *Journal of Power Sources*, vol. 303, pp. 388–398, 2016.

[22] J. P. Hespanha, *Linear systems theory*. Princeton university press, 2018.

[23] Gurobi Optimization, LLC, "Gurobi Optimizer Reference Manual," 2021. [Online]. Available: https://www.gurobi.com